Title

Compression-induced structural and mechanical changes of fibrin-collagen composites

Authors

Kim, OV
Litvinov, RI
Chen, J
et al.

Publication Date

2017-07-01

DOI

10.1016/j.matbio.2016.10.007

Peer reviewed

HHS Public Access

Author manuscript

Matrix Biol. Author manuscript; available in PMC 2018 July 01.

Published in final edited form as:

Matrix Biol. 2017 July ; 60-61: 141–156. doi:10.1016/j.matbio.2016.10.007.

Compression-induced structural and mechanical changes of fibrin-collagen composites

O. V. Kim[a,b], **R. I. Litvinov**[a], **J. Chen**[c], **D. Z. Chen**[c], **J.W. Weisel**[a,*], and **M. S. Alber**[b,d,*]

[a]Department of Cell and Developmental Biology, University of Pennsylvania, Perelman School of Medicine, Philadelphia, PA 19104

[b]Department of Applied and Computational Mathematics and Statistics, University of Notre Dame, Notre Dame, IN 46556

[c]Department of Computer Science and Engineering, University of Notre Dame, Notre Dame, IN 46556

[d]Department of Medicine, Indiana University School of Medicine, Indianapolis, IN 46202

Abstract

Fibrin and collagen as well as their combinations play an important biological role in tissue regeneration and are widely employed in surgery as fleeces or sealants and in bioengineering as tissue scaffolds. Earlier studies demonstrated that fibrin-collagen composite networks displayed improved tensile mechanical properties compared to the isolated protein matrices. Unlike previous studies, here unconfined compression was applied to a fibrin-collagen filamentous polymer composite matrix to study its structural and mechanical responses to compressive deformation. Combining collagen with fibrin resulted in formation of a composite hydrogel exhibiting synergistic mechanical properties compared to the isolated fibrin and collagen matrices. Specifically, the composite matrix revealed a one order of magnitude increase in the shear storage modulus at compressive strains > 0.8 in response to compression compared to the mechanical features of individual components. These material enhancements were attributed to the observed structural alterations, such as network density changes, an increase in connectivity along with criss-crossing, and bundling of fibers. In addition, the compressed composite collagen/fibrin networks revealed a non-linear transformation of their viscoelastic properties with softening and stiffening regimes. These transitions were shown to depend on protein concentrations. Namely, a decrease in protein content drastically affected the mechanical response of the networks to compression by shifting the onset of stiffening to higher degrees of compression. Since both natural and artificially composed extracellular matrices experience compression in various (patho)physiological conditions, our results provide new insights into the structural biomechanics

Corresponding authors*: Mark Alber, PhD, University of Notre Dame, Department of Applied and Computational Mathematics and Statistics, Notre Dame, IN 46556, malber@nd.edu, Ph: 574-631-8371. John Weisel, PhD, University of Pennsylvania, Perelman School of Medicine, 1154 BRB II/III, 421 Curie Boulevard, Philadelphia, PA 19104-6058, weisel@mail.med.upenn.edu, Ph: 215-898-3573.

of the polymeric composite matrix that can help to create fibrin-collagen sealants, sponges, and tissue scaffolds with tunable and predictable mechanical properties.

Keywords

fibrin; collagen; fibrin-collagen composites; compression; viscoelasticity; structural properties

Introduction

Collagen and fibrin are two major components of extracellular matrix providing structural integrity and mechanical strength to various tissues in the body, and they are present together in wounds. These biopolymers are also employed medically as safe, versatile and clinically applicable biomaterials. They have been effectively used separately [1–6] as well as in combination as fibrin-collagen composites [7–14] for various biomedical applications [2–4; 15], [16; 17]. Studying mechanical and structural properties of fibrin-collagen composites has a great practical significance, as they were shown to serve as effective hemostatic seals [13].

Addition of collagen to the fibrin hydrogel was shown to provide extra stiffness and durability [8; 18]. In addition to improved elasticity, composite fibrin-collagen matrices were shown to be permissive to endothelial network formation *in vitro* [8] and *in vivo* [9], providing support for their use instead of purified collagen and fibrin.

Individual collagen and fibrin matrices have been extensively characterized in terms of their mechanical response to shear and tensile load, yet little work has been done on studying their compressive behavior [19–25]. Both biopolymers self-assemble into thick fibers via hydrophobic and electrostatic interactions [26] to form three-dimensional filamentous networks with mechanical properties that are substantially different from those of synthetic polymers [25; 27]. Both biopolymers are known to exhibit a highly nonlinear stress-strain response known as strain-stiffening when exposed to tension or shear [22; 28–33]. This nonlinearity was suggested to originate from stiffening of individual fibers and redistribution of the load over the entire network, as well as some structural rearrangements [28; 34–36]. In contrast to the hydrogels made of pure proteins, much less is known about the mechanics of fibrin-collagen composites. It was shown that the fibrin-collagen mixture was several-fold stiffer than its components [37] and the interactions between components can be described in terms of series and parallel-type of network connections with transition to parallel type as the collagen content increased [18]. The linear modulus and toughness of tubular vascular constructs made of fibrin-collagen mixtures was also increased compared to collagen and fibrin alone [7].

There are only a few studies of compressive mechanics and structural rearrangements of these bio-composites, although compression of fibrin-collagen biomaterials occurs under various *in vivo* conditions, such as heart or limb muscle contraction, blood clot retraction, tendon or ligament reconstruction and controlling hemostasis in cardiovascular and hepatic surgery. Both unconfined and confined compression were previously used to increase the density and elasticity of separate collagen and fibrin matrices in order to assist in fabrication

of tissue analogous implants [38]. In particular, plastic compression of collagen was used to rapidly generate tissue scaffolds of optimal density to support myocyte contractility [39]. Viscoelastic properties of compressed fibrin were studied in [40; 41], highlighting a non-linear mechanical response to compression attributed to structural alterations of the matrix.

In the current paper, we studied structural and mechanical changes in the combined fibrin-collagen polymeric networks in response to controlled compression. We have shown that the composite fibrin-collagen matrix exhibits compressive viscoelastic and poroelastic properties that are different from the properties of its individual components. This distinction was attributed to structural alterations during simultaneous gelation of collagen and fibrin, leading to increased connectivity of the resultant network. These results provide mechanical and mechanistic bases for better understanding both the similarities and distinctions of the combined fibrin-collagen networks from their pure components to advance their usage as versatile biomaterials.

Results

A. Mechanical responses to compression of fibrin-collagen composite and its separated fibrin and collagen components

Changes in viscoelastic properties of the fibrin-collagen composite during compression—Mechanical response of fibrin-collagen composite exhibited remarkable softening-stiffening transitions as the compressive strain increased (Figure 2A). First, its elastic modulus decreased 4.6-fold at γ=0.3 (softening), remained relatively constant up to a compressive strain γ =0.82 (plateau), and increased 4.5-fold (stiffening) at a maximal compression at γ =0.99. There were significant differences in the elasticity and viscosity of fibrin-collagen matrices compared to pure collagen and fibrin gels. The shear storage modulus (G') of a fibrin-collagen construct was larger than that measured for its components alone over the whole range of compression degrees. The initial stiffness (G') of the fibrin-collagen composite was 1.5-times higher than the sum of the elastic moduli for pure collagen and fibrin gels. This difference decreased as the compressive strain increased up to γ=0.8, but then displayed a marked (more than 7-fold) increase at γ>0.9. Thus, the fibrin-collagen composite was initially stiffer than its individual components and was more responsive to compression than either fibrin or collagen alone.

Changes in the loss modulus (G'') of the fibrin-collagen constructs followed the same trend as the shear storage modulus (Figure 2B). First, it decreased 3-fold at γ=0.2, revealed a relative plateau up to γ=0.82, and displayed a marked 8.2-fold increase at a maximal compression degree. However, the composite material had a higher loss modulus than collagen and fibrin alone over the entire range of compression degrees. It was initially 2.5-fold larger than the sum of fibrin and collagen loss moduli. This difference was minimal in a plateau regime at γ=0.7 and increased 4.3-fold under a high compression degree at γ >0.9.

To assess relative viscosity and elasticity of compressed fibrin-collagen composite matrices, the phase angle, $\tan(\delta)=G''/G'$, was calculated. As shown in Figure 2C, the phase angle of the composite as well as its components (fibrin, collagen) revealed a slight or no increase up to γ=0.85 of compressive strain, but changed nonlinearly at higher compression degrees,

indicating a relative increase of viscosity over elasticity. When estimated over the entire range of compression degrees from γ=0 up to γ=0.99, the fibrin-collagen networks had the δ values ~1.7-fold larger than fibrin alone but not higher than collagen.

Viscoelastic properties of compressed fibrin and collagen gels at different protein concentrations

Storage Modulus: Both fibrin clots and collagen polymers with different protein densities displayed qualitatively similar elastic behavior in response to compression with softening-stiffening transitions as the degree of compression increased (Figure 3A, D). However, there were quite distinct differences in dynamic elasticity of the matrices in the undiluted and diluted samples. First, in the low protein concentration matrices, the initial value of the storage modulus G' was initially 7.4- and 1.7-times smaller than that of the higher protein concentration constructs of PPP-clots and collagen respectively. Second, the storage modulus of diluted matrices remained relatively constant (plateau) within almost the entire range of γ except its initial and the final portions revealing softening and stiffening transitions. Softening in the fibrin and collagen matrices with lower protein concentrations was observed at $\gamma < 0.1$ as G' dropped 3.7-fold and 4.4-fold, respectively. Stiffening of the compressed constructs occurred at $\gamma > 0.9$ as the storage modulus increased 12.3-fold in collagen and only 1.5-fold in fibrin matrices.

Compressed fibrin and collagen matrices of higher protein concentrations also softened at small $\gamma < 0.1$, but stiffened dramatically revealing > 100-fold increase of G' in fibrin clots and almost a three orders of magnitude increase in the collagen stiffness at $\gamma > 0.9$. In other words, the diluted matrix polymers were much weaker initially and less elastically responsive to compression compared to the fibrin and collagen polymers with a higher protein density.

Loss Modulus: The loss modulus, G'' of the studied polymers behaved qualitatively quite similar to their elastic components, revealing regions of modulus decrease, plateau and increase (Figure 3B, E). The networks with lower protein concentrations initially displayed a smaller G'' value than the more concentrated gels. In the clots formed from diluted PPP, the loss modulus decreased 3-fold at $\gamma = 0.2$ (vs 4-fold decrease in undiluted PPP-clot), remained relatively constant up to a compressive strain of $\gamma = 0.82$, and increased 8.2 times (vs >10-fold increase in undiluted PPP-clot) at a maximal compressive strain of $\gamma = 0.99$, which was ≈400-fold lower than the viscosity of the fully compressed gel prepared from the undiluted plasma. For the collagen at 2.5 mg/mL protein concentration the loss modulus almost did not change at $\gamma = 0.1$ and then began growing with almost 1,000-fold increase at $\gamma = 0.9$. Yet, in the construct with a lower protein density (1.5 mg/mL), the loss modulus decreased 4-fold at $\gamma = 0.1$ and remained almost constant up to $\gamma = 0.8$, after which it rapidly increased 17-fold at a maximal compressive strain $\gamma = 0.99$, which was ≈90-fold smaller than the loss modulus of the fully compressed collagen at a higher protein concentration.

Phase angle—As shown in Figure 3C, for both types of clot the phase angle ($\tan(\delta) = G''/G'$) changed nonlinearly as a function of compressive strain with a remarkable

quantitative difference in the dynamic viscoelasticity. The phase angle did not change significantly up to $\gamma = 0.8$ when it revealed a rapid up to 3-fold increase (Figure 3C, F). Over the entire range of compression degree, the less concentrated matrices had 2.3-and 1.2-fold smaller δ values in fibrin and collagen, respectively, indicating that the energy dissipative mechanisms (plasticity or viscosity) were less pronounced in the gels with lower protein densities. Meanwhile, at high compressions, larger dissipation can be expected as the fiber density increases dramatically.

Changes of the normal stress during compression of fibrin-collagen network and its components—As the fibrin-collagen matrix was compressed, the axial (normal) force on the upper rheometer plate was measured for each compressive strain. The normal stress calculated as the force distributed over the plate area revealed a highly nonlinear behavior (Figure 4). At the beginning of compression, the normal stress rose sharply, then relaxed, exhibiting a plateau, and finally increased dramatically at high degrees of compression. While the fibrin and collagen components indicated only a moderate increase in the normal stress (not exceeding one order of magnitude), the fibrin-collagen composites revealed a drastic increase of the normal stress (almost two orders of magnitude) at $\gamma > 0.9$. Remarkably, the normal stress response of the fibrin-collagen composite to the strain was significantly (up to 13.5-fold) higher than the sum of the individual values for fibrin and collagen. Since the normal stress-strain behavior is governed by the flow of interstitial fluid through network pores, the large values of the normal stress in the fibrin-collagen composite indicate a significant reduction in liquid permeability and an increase in polymer density at the higher strains.

B. Structural changes in fibrin-collagen composites and fibrin and collagen networks during compression

Ultrastructural changes: Fibrin-collagen composite networks revealed a mixture of individual fibers and fiber bundles having an average thickness (M±SD) of 85±12 nm and 283±82 nm, respectively (Figure 5). With respect to the fibrin-collagen components, pure collagen networks consisted of entangled individual fibers with 77±12 nm average diameter as well as twisted fiber bundles having an average thickness of 258±73 nm. Similar to the fibrin-collagen and collagen matrices, pure fibrin networks were composed of entangled fibers approximately 89±21 nm in diameter and 391±158-nm thick fiber bundles. Fibrin fiber bundles consisted of loosely twisted fibers with larger inter-fiber porosity compared to collagen, suggesting that the collagen bundles were more compacted than fibrin fiber bundles. This could contribute to the greater thickness of fibrin bundles over collagen. The highest spatial density of bundles was achieved in fibrin-collagen matrices (0.07±0.02 bundles/μm^2), while in the fibrin networks the bundle density was ~10 times smaller than that in collagen and was equal to 0.40±0.12 bundles/μm^2 vs 0.04±0.01 bundles/μm^2, respectively.

Structural changes observed by light microscopy

Network densification: Analysis of reconstituted 3D structures of the compressed fibrin-collagen matrices and their separate components imaged via confocal light microscopy

(Figure 6, Figure S6) revealed buckling and bending of individual fibers as well as densification of the networks. We quantified changes in the network density by measuring the number of nodes per volume. By comparing the uncompressed and two-fold compressed networks we revealed a 20% node density increase in fibrin, 40% in collagen, and 33% in fibrin-collagen matrices (Figure 7A).

Branching of fibers (oblique contacts): To analyze topological differences of all three types of networks, we quantified the connectivity of the networks by measuring the number of fibers (n=3 to n=6) radiating from a network node and calculating the relative node density $\rho(n)/\rho_T$. In addition, we calculated the apparent branching degree n* (average connectivity) for the networks studied (see Materials and Methods section). Typically, three fibers forming a visible branching point or a node (n=3) prevailed over 4-, 5-, and 6-degree nodes in all types of networks. The variability in the number of fibers in branch points are shown in Figure 7B: 60–75% of the nodes had n=3; 20–27% had n=4; 4–13% of the nodes had n=5; and 2% to 4% of the nodes had n=6.

However, in the compressed matrices, the relative density of the higher degree nodes (n>3) increased due to formation of new fiber connections caused by oblique contacts or crisscrossing of fibers with a corresponding decrease of nodes connecting three fibers (n=3).

Combined networks demonstrated a significantly lower fraction of 3-degree nodes than networks made of either fibrin or collagen. In uncompressed fibrin and collagen networks the density of 3-degree nodes was higher by 14–20% than in the fibrin-collagen composite, while the summarized density of 4-, 5-, and 6-degree nodes in the composite network was larger by 16–54% and 47–400% than in individual fibrin and collagen matrices, respectively. In compressed networks the corresponding relative changes were 10–37%, 11–64%, and 25–344%. As a result, the degree of branching (average connectivity), n*, of uncompressed fibrin-collagen composites was higher than the connectivity of fibrin and collagen: $n^*_{fib}=3.29\pm0.3$, $n^*_{coll}=3.45\pm0.4$, and $n^*_{coll\text{-}fib}=3.55\pm0.5$ (a two-tailed Mann-Whitney test, $P<0.05$, $n=1078$, when compared to collagen). Compression of matrices yielded an increased connectivity in all matrices as shown in Table S1.

Reconstituted three-dimensional images revealed that interaction of collagen and fibrin fibers occurred via crisscrossing of fibers as well as due to formation of fiber bundles, but not via copolymerization (Figure 8). These types of fiber-fiber interactions can partially explain the synergistic mechanical response of composite scaffolds when compared to responses of its components.

Thus, composite fibrin-collagen materials revealed network structure with a higher average connectivity than collagen and fibrin alone due to oblique fiber contacts as well as fiber bundling.

Fibrin network structure in the presence of collagen: In order to delineate possible structural changes in the fibrin network due to the presence of collagen in the construct, we have analyzed and compared fibrin networks formed from diluted plasma and in the presence of collagen (Figure 9). To that end, we calculated the absolute node density $\rho(n)$ as

a function of branching degree, n, and found that fibrin network in the composite revealed slightly higher values of the apparent branching degree: n^* = 3.45 (in fibrin-collagen composite) vs. 3.29 (in fibrin, $p<0.05$). Meanwhile, the absolute total node density ρ_T of the fibrin network in the fibrin-collagen composite was significantly larger (11 fold) than that in the fibrin network alone. In the same time, confocal images indicated that fibrin fibers in the construct were 1.5 times thinner that fibers in a pure fibrin network. Thus, in the presence of collagen, polymerized fibrinogen forms a network of higher node density, thinner fibers and with increased branching degree.

Segment Length: Measurements of the fiber segment lengths in the constructs revealed that fibrin networks of diluted plasma have significantly larger fiber segment length variation than that in collagen (Figure 10). The mean and median values of fiber segments were also higher in fibrin network than in collagen. The mean segment length in fibrin networks, reached 410 nm (lower quartile, Q_1=196 nm, upper quartile Q_2=567 nm). In collagen matrices it was ~205 nm (Q_1 = 137 nm, Q_2 = 248 nm) and in the mixed scaffold the mean segment length was ~315 nm (Q_1 = 208 nm, Q_2 = 441 nm). Similarly, the variation of fiber segment length and the median fiber length in the fibrin-collagen constructs revealed intermediate values lying in between the corresponding metrics for fibrin and collagen matrices. The mean lengths and variations were slightly (up to 6%) lower in compressed collagen, fibrin and fibrin-collagen matrices (two-tailed Mann-Whitney test, $P<0.05$, a significant difference when compared to the uncompressed matrices).

Discussion

Gels based on gelatin, collagen, fibrin or elastin have been used as scaffolds [42] to optimize cellular activities, including differentiation, proliferation, and changes in morphology [43; 44]. Fibrin has been frequently used *in vivo* as it plays a key role in hemostasis and wound healing and *in vitro* for engineering of provisional matrices [23]. However, an uncompressed fibrin network can be too soft to withstand large forces, which can strongly limit its use in tissue engineering [45]. To see if the mechanical properties of the composite fibrin-collagen material can be modified by applying the external unconfined compression and varying protein density, we examined relationships between the network structure and bulk mechanical properties of compressed fibrin-collagen composites and their components.

Structural mechanics of fibrin-collagen composite

Correlation between fibrin and collagen microstructure and their overall mechanical response was previously studied by Lai et al. [37]. In this work the mechanical behavior of fibrin, collagen and their composites were tested by applying a tensile load to gel rings up to their failure, whereas we examined shear elasticity of gradually compressed matrices. Similar to our results, the authors demonstrated that the structure of the components in mixtures differed from that of individual matrices. To distinguish structural peculiarities of fibrin-collagen components, Lai et al. used enzymes to digest fibrin and collagen in co-gels, whereas we distinguished fibrin and fibrin-collagen networks using two distinct modes of confocal microscopy. The authors showed that co-gelation of collagen with fibrin from purified fibrinogen yielded longer but thinner fibers. By contrast, our study revealed

intermediate thicknesses and lengths of fibers in co-gels, with shorter fibrin fibers when compared to collagen and fibrin matrices alone. Our connectivity analysis is only partially in agreement with [37], and reveals a higher degree of connectivity in the composite. These morphological discrepancies might be due to the differences in gelation conditions, such as variation in pH, the use of purified fibrinogen versus human plasma, which could affect fibril organization. Polymerization temperature is another parameter that can affect structural and mechanical properties of fibrin and collagen matrices [46]. This suggests that properties of the fibrin-collagen composite would vary with the polymerization temperature: matrices formed at a lower temperature would contain thicker fibers and larger pores than the matrices polymerized at higher temperatures. Mechanical characteristics of fibrin-collagen matrices would be also affected and stiffer matrices with higher responsiveness to compression should be expected at higher temperatures.

One of the major reasons that the mechanical properties of the mixture are synergistic rather than additive is that gelation of fibrin in the presence of collagen results in a fibrin network of a more complex topology than that of pure fibrin. In addition, criss-crossing of fibrin and collagen fibers can occur along with crisscrossing of fibrin-fibrin and collagen-collagen fibers, and the composite network has a greatly increased total fiber density, which correlated with the enhancement in the fibrin-collagen matrix stiffness. Both scanning electron microscopy and laser confocal microscopy of the networks revealed the presence of fiber bundles coexisting with individual fibers. Similar hierarchical ultrastructure was observed in [47], indicating formation of bundles in fibrin-collagen matrices. Formation of fiber aggregates (bundles) must have direct consequences for the viscoelastic properties of the matrix as thick fiber bundles can sustain higher stress values and hence enhance stiffness of the whole network as well as its response to compression.

Conceivably, direct interaction between the two polymers could also contribute to an increase in elasticity of the co-networks, although it is not quite clear how fibrin and collagen interact at the molecular level. Previous studies suggested a direct role for Factor XIIIa in the Ca^{2+}-dependent binding of fibrin and collagen, leading to the formation of covalent cross-links between the two proteins [48]. Moreover, direct molecular interaction between the two fibrous proteins was propounded in [49], who pointed out that fibrinogen/fibrin competes with fibronectin and matrix metalloproteinase-1 for the same binding site(s) on collagen fibers. In compressed scaffolds, along with strong covalent bonds between fiber segments of the originally uncompressed network, additional non-covalent interactions may occur between criss-crossed fibers, leading to a stiffening regime at higher compressive strains ($\gamma > 0.8$ in Figure 2). Although sliding between entangled fibers in pure components are expected, presumably, such interactions between collagen and fibrin are different from those occurring in fibrin and collagen gels alone, therefore affecting the stress-strain response of compressed co-networks [40]. Thus, both increased structural complexity of fibrin-collagen networks, possible covalent cross-linking and additional relatively weak non-covalent interactions might contribute to the mechanical properties of compressed composites.

Normal stress as a function of compressive strain in the collagen/fibrin networks

The observed changes in normal stress during unconfined compression under vertical load must be determined by extrusion of the interstitial fluid through matrix pores [41; 50; 51]. Unlike in confined compression, which conserves fluid volume and fluid incompressibility prevents the network from collapse, in unconfined compression the liquid is squeezed out of the gel resulting in significant changes of gel composition [38]. In our experiments, the changes in normal stress during compression of fibrin-collagen composite and polymerized collagen revealed three distinct regions (linear increase, plateau, followed by a dramatic increase at large γ), which is similar to what was observed earlier in fibrin clots [41]. However, the composite material was characterized by a non-additive (synergistic) normal stress curve compared to fibrin and collagen alone, which is probably due to a nonlinear decrease of the network pore size, leading to reduction in gel permeability. Indeed, our estimates show that in compressed gels permeability is significantly reduced during compression (up to several orders of magnitude) in the composite matrix as well as its pure components (Supplementary Figure S7). As the fibrous matrix is compressed, one might expect that off-axis stresses are present in the network structure. It is highly likely that these stresses dissipate during expulsion of water which is indirectly reflected by Supplementary Figure S8, showing relaxation of the normal stress after each compression step reaching equilibrium. This indicates that the net off-axis stress tends to zero at equilibrium at low and moderate strains and slowly dissipates at high strains.

Viscoelastic and structural properties of collagen/fibrin networks

Both fibrin and collagen are known to display strain-hardening in response to a tensile load [22; 28; 31; 32]. In addition, fibrin was shown to stiffen under compression at high strains [40]. Strain-hardening can be biologically important as it permits fibrin clots to be compliant at low strains but then make them stiffer at large deformations to avoid clot damage and emboli formation. In collagen, strain-stiffening may contribute to cell and tissue integrity under mechanical deformations [30]. Both materials also indicate viscoelastic properties under shear or compression, as they are able to recover deformations as well as to relax internal stresses via dissipation [31; 40; 52]. Additionally, when exposed to repeating large-shear-strain loading, these biopolymers are characterized by a shift of the nonlinear stress response to higher strains due to lengthening of individual fibers [53] associated with interplay between bending and buckling of fibers.

In addition to what has been previously shown for compressed fibrin [40; 41], in this work we have demonstrated that collagen networks were similar to fibrin in their highly non-linear mechanical response to compression with stiffening at high compression strains. Since the rheometry was performed using parallel plate geometry, the apparent properties of the hydrogels studied could be affected by the underlying highly stiff materials. However, there are at least four arguments that make these artefactual effects unlikely in our study. First, the gel stiffening was observed at strains of about 0.8 and smaller; second, the points of strain-stiffening were distinct for each of the three hydrogels studied; third, the strain-stiffening for each hydrogel depended on the protein density and occurred at much lower strains in diluted samples that would not be expected if the stiffening originated from the stiff substrate below the samples; fourth, we observed a phase boundary in compression of these samples: there is

a densified phase at the top and a rarefied phase at the bottom, which is the same as the uncompressed matrix, indicating that there is no effect of the stiff substrate below the samples.

The effects of fibrin and collagen concentrations on network polymerization have been previously studied in detail [54; 55]. According to these studies, as the concentration of protein decreases, thicker fibers with a more open network are formed, which is in agreement with our observations (Figure S2). While collagen type I networks exposed to shear revealed a surprising concentration-independence of the network stiffness [56] we showed that the softening-stiffening transition of both fibrin and collagen polymers significantly depends on the protein concentration: networks formed at a higher protein content were more responsive to compression (shifting the stiffening regime to smaller strains) followed by shortening of the elasto-plastic plateau.

These findings are important for bioengineering applications, as they indicate that mechanical response of collagen- and fibrin-based matrices can be modulated by varying protein density. Uncompressed patches can be readily formed by following the standard protocol using commercial fibrin-collagen assays (for example, TachoSil Co.). Once the gel is formed, matrix stiffness can be further modified by applying mild or high compression to produce softer or harder fibrin-collagen patches to adjust for the mechanotype of a specific tissue. Furthermore, as we showed previously, by controlling the compression rate, matrices of nonuniform densities varying in the z-direction can be created [41]. This can be advantageous in designing fibrin-collagen scaffolds that permit cell infiltration and at the same time exhibit high mechanical strength [57].

Conclusions

In response to compression, the fibrin-collagen composites reveal a unique mechanical behavior characterized by a dual softening-stiffening transition as the degree of compression increases. Both uncompressed and compressed fibrin-collagen networks have elastic properties that are enhanced over pure collagen or fibrin matrices. The synergistic mechanical behavior of the compressed fibrin-collagen composite is caused by the structural alterations due to changes in the course of gelation of co-networks associated with increased node density and average connectivity as well as formation of additional contacts between collagen and fibrin fibers. Changing protein density in the collagen and fibrin constructs alters the stress-strain relationship by shifting the onset of stiffening to lower compressive strains as the protein density increases. Our results provide fundamental mechanical and structural characteristics of these composite matrices that are important for designing versatile fibrin- and collagen-based biomaterials as well as understanding and predicting their responses in wounds to naturally occurring or artificial compressive deformations.

Materials and Methods

Fibrin

Fibrin polymer was formed by adding human α-thrombin (0.5 U/mL final concentration, Enzyme Research Labs) and $CaCl_2$ (40 mM final concentration) to once frozen and thawed

pooled human citrated platelet-poor plasma (PPP) obtained from platelet-rich plasma by centrifugation at 2000g, 30 min, at room temperature. Blood was obtained from 9 healthy volunteers with informed consent and approval by the University of Pennsylvania IRB. The concentration of fibrin formed in normal plasma is almost equal to the concentration of fibrinogen (2–3.5 mg/mL), since under the conditions of our experiments, all soluble fibrinogen is converted to insoluble fibrin. All procedures were carried out in accordance with the approved guidelines. To form fibrin networks with a higher porosity, part of the PPP was diluted 2-fold with phosphate buffered saline (PBS), pH 7.4. Thrombin-activated undiluted or diluted PPP samples were placed in a gap between preheated at 37°C horizontal rheometer plates separated by a distance of 410 μm. Plasma (600 μl) was allowed to clot for 1 hour before compression and rheological measurements were started. Throughout the experiment, a piece of wet filter paper was kept around the rheometer plates and periodically (each 20–30 minutes) sprayed with water to prevent sample drying. Three fibrin clots from undiluted PPP and three clots from diluted PPP were prepared as described and analyzed in parallel at the same experimental conditions.

Polymerized collagen

Collagen type I, from rat tail (telocollagen, 4 mg/mL in 0.02 N acetic acid, 90% purity, Corning Inc.) was mixed with pre-chilled 10x PBS, 1 N NaOH, and water on ice to make the final collagen concentration 1.5 mg/mL or 2.5 mg/mL in 1x PBS at pH 7.5. The gel of collagen (620 μL) was allowed to form for 1 hour between preheated at 37°C horizontal rheometer plates separated by a distance of 410 μm prior to compression and rheological measurements. During collagen polymerization and measurements, the sample drying was prevented as described for fibrin. Three collagen samples at 1.5 mg/mL and three samples at 2.5 mg/mL were prepared as described and analyzed in parallel at the same experimental conditions.

Fibrin-collagen mixture

Fibrin-collagen composite gels were formed by adding human α-thrombin (0.5 U/mL final concentration) to a mixture of a pooled human citrated PPP and 3.5 mg/mL rat tail collagen I solution (prepared as described previously) in the presence of $CaCl_2$ (40 mM final concentration) to get a final concentration of collagen of 1.5 mg/mL. 620 μL of fibrin-collagen constructs were formed at 37°C between rheometer plates separated by a distance of 410 μm for 1 hour to ensure the covalent cross-linking of fibrin by factor XIIIa and complete collagen polymerization. During formation of the construct and rheological measurements, sample drying was prevented as described. Nine fibrin-collagen composite samples were prepared and used for compression studies with combined structural and rheological examination.

Uniaxial compression of fibrin-collagen constructs

Fibrin, collagen, and fibrin-collagen gels were compressed using a computer-controlled AR-G2 Rheometer (TA Instruments, New Castle, DE) (Figure 1). 410-μm-thick fresh hydrated gels were formed directly between the rheometer plates and compressed vertically down to more than 1/10 of their initial thickness. Compression of the constructs was performed in a

stepwise manner with 20-μm steps at the rate of 30 μm/s, as the upper rheometer plate exerted a downward force on the top surface of the clot.

To visualize uncompressed and compressed polymer networks, separate compression experiments were performed, in which 120-μm-thick fibrin, collagen, and fibrin-collagen gels were formed in a flow chamber built of a microscope glass slide (bottom) and a glass cover slip (top) separated by a highly plastic putty adhesive material. The chamber was compressed by applying vertical pressure on the cover slip using the upper rheometer plate. Due to high plasticity of the adhesive spacer (forming the lateral walls of the chamber), gels within the chamber were compressed irreversibly as the cover slip was moved downward. The fully polymerized and cross-linked plasma clots, collagen gels and their mixture were compressed by 50% of their initial thickness followed by confocal microscopy. A compressive strain (γ) was defined as the absolute fractional decrease in fibrin clot thickness $\gamma = |\Delta L/L_0|$, where $\Delta L = L - L_0$, and L_0 and L are the initial and reduced thickness dimensions of the uncompressed and compressed clots, respectively.

Oscillatory shear rheometry of compressed constructs

Changes in viscous and elastic properties of fibrin, collagen, and fibrin-collagen gels at each step of compression were examined via oscillatory rheometry using a AR-G2 Rheometer (TA Instruments, New Castle, DE) operating in a 20 mm parallel plate configuration. The gels were probed by continuously oscillating the sample at a fixed 0.5% strain amplitude and at a frequency of 1 Hz to assure a linear stress-strain response to imposed shear. The strain-controlled oscillatory shear deformation was initiated immediately after each subsequent step of compression and lasted for two minutes. The storage modulus, G′, of the compressed construct represented the stored energy and characterized the elastic response of the gel to applied shear. It is defined as $G' = (\tau_0/\gamma_0)\cos(\delta)$, where, γ_0 is a strain amplitude (as small as 0.5%), τ_0 is a shear stress amplitude, and δ is a phase shift in the shear stress with respect to applied oscillatory strain. The shear loss modulus, G″, which characterizes the viscous response of the gel and is associated with energy dissipation, is calculated as $G'' = (\tau_0/\gamma_0)\sin(\delta)$.

Scanning electron microscopy

Following rheological measurements, the compressed networks were transferred into Petri dishes and washed three times with a physiological buffer [20 mM (4-(2-hydroxyethyl)-1-piperazineethanesulfonic acid - HEPES, 150 mM NaCl, pH 7.4] and 50 mM sodium cacodylate buffer, pH 7.4, over several hours. The samples were fixed in 2% glutaraldehyde, dehydrated in ethanol, dried with hexamethyldisilazane, and sputter coated with gold-palladium. Nine samples (three of each type) were examined using FEI Quanta 250 scanning electron microscope (FEI, Hillsboro, OR) at intermediate (10,000–100,000X) and high (>100,000X) magnification levels (Figs. S2 and S3).

Confocal microscopy

To visualize fibrin network structure using fluorescent confocal microscopy, Alexa-Fluor 488-labeled human fibrinogen (Molecular Probes, Grand Island, NY) was added to PPP before clotting at a final concentration of 0.04 mg/mL. To image the collagen network

reflectance confocal microscopy was used. Uncompressed and compressed fibrin, collagen, and fibrin-collagen networks were formed inside flow chambers as described previously. The networks were imaged using Zeiss LSM710 laser scanning confocal microscope to generate high resolution z-stack images spanning 100 μm of the sample thickness. We used a Plan Apo 40x water immersion objective lens (NA 1.2). An argon laser beam with a 488-nm wave length was used for fluorescent confocal microscopy of labeled fibrin and for reflectance imaging of unlabeled collagen networks. The z-stack distance between slices was set as 0.5 μm with a 1024x1024 pixels resolution for each slice.

Image analysis

A two-stage scheme to extract and analyze the structure of networks in 3D confocal microscopy images was utilized. First, segmentation of networks using the input image stack was performed. Second, identification of the topological and morphological structures was done via representation of the network as an augmented graph (Supplementary Figure S1). Using the graph representation obtained, further quantitative analysis of the networks including node density, fiber length and thickness distributions was performed. The details of the network reconstruction algorithm and structure quantification can be found in our previous work [58]. Analysis of the networks in confocal z-stacks was limited by the resolution and performed for uncompressed and intermediately compressed (γ=0.5) networks. Highly compressed (γ>0.9) dense networks were analyzed in scanning electron microscopy images. Fiber diameter was measured manually in 36 images obtained from at least three gels using ImageJ and subsequent statistical analysis was performed using MATLAB.

Characterization of fiber branching

The network node connectivity distribution function was defined as, $\rho^*(n)=\rho(n)/\rho_T$, where $\rho(n)$ is the absolute node number density with a branching degree n, and $\rho_T=\sum_{n=1}^{6}\rho(n)$ is the absolute total density of nodes with the branching degrees from 1 to 6. The apparent branching degree (average connectivity) $n^*=\sum_{n=1}^{6}n\rho(n)/\rho_T$, was evaluated as the number of fibers (n) radiating from the node (n=3 through n=6).

Supplementary Material

Refer to Web version on PubMed Central for supplementary material.

Acknowledgments

We would like to acknowledge support from the National Institutes of Health grants NIH 1U01HL116330 (OVK, RIL, JWW, and MSA) and HL090774 (RIL and JWW), NSF Grant CCF-1217906 (DZC) and Walter Cancer Foundation (OVK).

References

1. Lee CH, Singla A, Lee Y. Biomedical applications of collagen. Int J Pharm. 2001; 221:1–22. [PubMed: 11397563]

2. Drury JL, Mooney DJ. Hydrogels for tissue engineering: scaffold design variables and applications. Biomaterials. 2003; 24:4337–4351. [PubMed: 12922147]
3. Auger F, Rouabhia M, Goulet F, Berthod F, Moulin V, Germain L. Tissue-engineered human skin substitutes developed from collagen-populated hydrated gels: clinical and fundamental applications. Medical and Biological Engineering and Computing. 1998; 36:801–812. [PubMed: 10367474]
4. Sela J, Kaufman D, Shoshan S, Shani J. Retinoic acid enhances the effect of collagen on bone union, following induced non-union defect in guinea pig ulna. Inflammation Res. 2000; 49:679–683.
5. Sato H, Kitazawa H, Adachi I, Horikoshi I. Microdialysis assessment of microfibrous collagen containing a P-glycoprotein-mediated transport inhibitor, cyclosporine A, for local delivery of etoposide. Pharm Res. 1996; 13:1565–1569. [PubMed: 8899852]
6. Minabe M, Takeuchi K, Tamura T, Hori T, Umemoto T. Subgingival administration of tetracycline on a collagen film. J Periodontol. 1989; 60:552–556. [PubMed: 2810009]
7. Cummings CL, Gawlitta D, Nerem RM, Stegemann JP. Properties of engineered vascular constructs made from collagen, fibrin, and collagen–fibrin mixtures. Biomaterials. 2004; 25:3699–3706. [PubMed: 15020145]
8. Rao RR, Peterson AW, Ceccarelli J, Putnam AJ, Stegemann JP. Matrix composition regulates three-dimensional network formation by endothelial cells and mesenchymal stem cells in collagen/fibrin materials. Angiogenesis. 2012; 15:253–264. [PubMed: 22382584]
9. Rao RR, Ceccarelli J, Vigen ML, Gudur M, Singh R, Deng CX, Putnam AJ, Stegemann JP. Effects of hydroxyapatite on endothelial network formation in collagen/fibrin composite hydrogels in vitro and in vivo. Acta biomaterialia. 2014; 10:3091–3097. [PubMed: 24657675]
10. Nomori H, Horio H, Suemasu K. Mixing collagen with fibrin glue to strengthen the sealing effect for pulmonary air leakage. Ann Thorac Surg. 2000; 70:1666–1670. [PubMed: 11093507]
11. Prior JJ, Wallace DG, Harner A, Powers N. A sprayable hemostat containing fibrillar collagen, bovine thrombin, and autologous plasma. Ann Thorac Surg. 1999; 68:479–485. [PubMed: 10475416]
12. Colombo GL, Bettoni D, Di Matteo S, Grumi C, Molon C, Spinelli D, Mauro G, Tarozzo A, Bruno GM. economic and outcomes consequences of TachoSil®: a systematic review. Vascular health and risk management. 2014; 10:569. [PubMed: 25246797]
13. Wagner WR, Pachence JM, Ristich J, Johnson PC. Comparativein VitroAnalysis of Topical Hemostatic Agents. J Surg Res. 1996; 66:100–108. [PubMed: 9024819]
14. Low RK, Moran ME, Goodnight JE Jr. Microfibrillar collagen hemostat during laparoscopically directed liver biopsy. J Laparoendosc Surg. 1993; 3:415–420. [PubMed: 8268517]
15. Sell SA, McClure MJ, Garg K, Wolfe PS, Bowlin GL. Electrospinning of collagen/biopolymers for regenerative medicine and cardiovascular tissue engineering. Adv Drug Deliv Rev. 2009; 61:1007–1019. [PubMed: 19651166]
16. Kasahara H, Hayashi I. Polyglycolic acid sheet with fibrin glue potentiates the effect of a fibrin-based haemostat in cardiac surgery. J Cardiothorac Surg. 2014; 9 121-8090-9-121.
17. Wechselberger G, Russell RC, Neumeister MW, Schoeller T, Piza-Katzer H, Rainer C. Successful transplantation of three tissue-engineered cell types using capsule induction technique and fibrin glue as a delivery vehicle. Plast Reconstr Surg. 2002; 110:123–129. [PubMed: 12087242]
18. Lai VK, Lake SP, Frey CR, Tranquillo RT, Barocas VH. Mechanical behavior of collagen-fibrin co-gels reflects transition from series to parallel interactions with increasing collagen content. J Biomech Eng. 2012; 134:011004. [PubMed: 22482659]
19. Ramachandran, GN. Treatise on collagen. Academic Press; 1967.
20. Randall J, Fraser R, Jackson S, Martin A, North A. Aspects of collagen structure. Nature. 1952; 169:1029–1033. [PubMed: 14941097]
21. Fratzl, P. Collagen: structure and mechanics. Springer Science & Business Media; 2008.
22. Brown AE, Litvinov RI, Discher DE, Purohit PK, Weisel JW. Multiscale mechanics of fibrin polymer: gel stretching with protein unfolding and loss of water. Science. 2009; 325:741–744. [PubMed: 19661428]
23. Bensaıd W, Triffitt J, Blanchat C, Oudina K, Sedel L, Petite H. A biodegradable fibrin scaffold for mesenchymal stem cell transplantation. Biomaterials. 2003; 24:2497–2502. [PubMed: 12695076]

24. Weisel JW. Fibrinogen and fibrin. Adv Protein Chem. 2005; 70:247–299. [PubMed: 15837518]
25. Janmey PA, Winer JP, Weisel JW. Fibrin gels and their clinical and bioengineering applications. J R Soc Interface. 2009; 6:1–10. [PubMed: 18801715]
26. Wood GC, Keech MK. The formation of fibrils from collagen solutions 1. The effect of experimental conditions: kinetic and electron-microscope studies. Biochem J. 1960; 75:588–598. [PubMed: 13845809]
27. Motte S, Kaufman LJ. Strain stiffening in collagen I networks. Biopolymers. 2013; 99:35–46. [PubMed: 23097228]
28. Piechocka IK, Bacabac RG, Potters M, MacKintosh FC, Koenderink GH. Structural hierarchy governs fibrin gel mechanics. Biophys J. 2010; 98:2281–2289. [PubMed: 20483337]
29. Wen Q, Basu A, Winer JP, Yodh A, Janmey PA. Local and global deformations in a strain-stiffening fibrin gel. New Journal of Physics. 2007; 9:428.
30. Storm C, Pastore JJ, MacKintosh FC, Lubensky TC, Janmey PA. Nonlinear elasticity in biological gels. Nature. 2005; 435:191–194. [PubMed: 15889088]
31. Nelb GW, Gerth C, Ferry JD, Lorand L. Rheology of fibrin clots: III. Shear creep and creep recovery of fine ligated and coarse unligated clots. Biophys Chem. 1976; 5:377–387. [PubMed: 974229]
32. Kurniawan N, Grimbergen J, Koopman J, Koenderink G. Factor XIII stiffens fibrin clots by causing fiber compaction. Journal of Thrombosis and Haemostasis. 2014; 12:1687–1696. [PubMed: 25142383]
33. Liu W, Jawerth LM, Sparks EA, Falvo MR, Hantgan RR, Superfine R, Lord ST, Guthold M. Fibrin fibers have extraordinary extensibility and elasticity. Science. 2006; 313:634. [PubMed: 16888133]
34. Kim E, Kim OV, Machlus KR, Liu X, Kupaev T, Lioi J, Wolberg AS, Chen DZ, Rosen ED, Xu Z. Correlation between fibrin network structure and mechanical properties: an experimental and computational analysis. Soft Matter. 2011; 7:4983–4992.
35. Hudson NE, Houser JR, O'Brien ET, Taylor RM, Superfine R, Lord ST, Falvo MR. Stiffening of individual fibrin fibers equitably distributes strain and strengthens networks. Biophys J. 2010; 98:1632–1640. [PubMed: 20409484]
36. Ryan EA, Mockros LF, Weisel JW, Lorand L. Structural origins of fibrin clot rheology. Biophys J. 1999; 77:2813–2826. [PubMed: 10545379]
37. Lai VK, Frey CR, Kerandi AM, Lake SP, Tranquillo RT, Barocas VH. Microstructural and mechanical differences between digested collagen–fibrin co-gels and pure collagen and fibrin gels. Acta biomaterialia. 2012; 8:4031–4042. [PubMed: 22828381]
38. Neel EAA, Cheema U, Knowles JC, Brown RA, Nazhat SN. Use of multiple unconfined compression for control of collagen gel scaffold density and mechanical properties. Soft Matter. 2006; 2:986–992.
39. Serpooshan V, Zhao M, Metzler SA, Wei K, Shah PB, Wang A, Mahmoudi M, Malkovskiy AV, Rajadas J, Butte MJ. The effect of bioengineered acellular collagen patch on cardiac remodeling and ventricular function post myocardial infarction. Biomaterials. 2013; 34:9048–9055. [PubMed: 23992980]
40. Kim OV, Litvinov RI, Weisel JW, Alber MS. Structural basis for the nonlinear mechanics of fibrin networks under compression. Biomaterials. 2014; 35:6739–6749. [PubMed: 24840618]
41. Kim OV, Liang X, Litvinov RI, Weisel JW, Alber MS, Purohit PK. Foam-like compression behavior of fibrin networks. Biomechanics and modeling in mechanobiology. 2015:1–16. [PubMed: 24718853]
42. Shevchenko RV, James SL, James SE. A review of tissue-engineered skin bioconstructs available for skin reconstruction. J R Soc Interface. 2010; 7:229–258. [PubMed: 19864266]
43. Dikovsky D, Bianco-Peled H, Seliktar D. The effect of structural alterations of PEG-fibrinogen hydrogel scaffolds on 3-D cellular morphology and cellular migration. Biomaterials. 2006; 27:1496–1506. [PubMed: 16243393]
44. Natesan S, Zhang G, Baer DG, Walters TJ, Christy RJ, Suggs LJ. A bilayer construct controls adipose-derived stem cell differentiation into endothelial cells and pericytes without growth factor stimulation. Tissue Engineering Part A. 2010; 17:941–953.

45. Shah JV, Janmey PA. Strain hardening of fibrin gels and plasma clots. Rheologica Acta. 1997; 36:262–268.
46. Raub CB, Suresh V, Krasieva T, Lyubovitsky J, Mih JD, Putnam AJ, Tromberg BJ, George SC. Noninvasive assessment of collagen gel microstructure and mechanics using multiphoton microscopy. Biophys J. 2007; 92:2212–2222. [PubMed: 17172303]
47. Rowe SL, Stegemann JP. Microstructure and mechanics of collagen-fibrin matrices polymerized using ancrod snake venom enzyme. J Biomech Eng. 2009; 131:061012. [PubMed: 19449966]
48. Duckert F, Nyman D. Factor XIII, fibrin and collagen. Suppl Thromb Haemost. 1978; 63:391–396. [PubMed: 262335]
49. Reyhani V, Seddigh P, Guss B, Gustafsson R, Rask L, Rubin K. Fibrin binds to collagen and provides a bridge for alphaVbeta3 integrin-dependent contraction of collagen gels. Biochem J. 2014; 462:113–123. [PubMed: 24840544]
50. Cohen B, Lai W, Mow V. A transversely isotropic biphasic model for unconfined compression of growth plate and chondroepiphysis. J Biomech Eng. 1998; 120:491–496. [PubMed: 10412420]
51. Mow VC, Kuei S, Lai WM, Armstrong CG. Biphasic creep and stress relaxation of articular cartilage in compression: theory and experiments. J Biomech Eng. 1980; 102:73–84. [PubMed: 7382457]
52. Knapp DM, Barocas VH, Moon AG, Yoo K, Petzold LR, Tranquillo RT. Rheology of reconstituted type I collagen gel in confined compression. Journal of Rheology (1978-present). 1997; 41:971–993.
53. Munster S, Jawerth LM, Leslie BA, Weitz JI, Fabry B, Weitz DA. Strain history dependence of the nonlinear stress response of fibrin and collagen networks. Proc Natl Acad Sci U S A. 2013; 110:12197–12202. [PubMed: 23754380]
54. Ho W, Tawil B, Dunn JC, Wu BM. The behavior of human mesenchymal stem cells in 3D fibrin clots: dependence on fibrinogen concentration and clot structure. Tissue Eng. 2006; 12:1587–1595. [PubMed: 16846354]
55. Raspanti M, Viola M, Sonaggere M, Tira ME, Tenni R. Collagen fibril structure is affected by collagen concentration and decorin. Biomacromolecules. 2007; 8:2087–2091. [PubMed: 17530890]
56. Licup AJ, Münster S, Sharma A, Sheinman M, Jawerth LM, Fabry B, Weitz DA, MacKintosh FC. Stress controls the mechanics of collagen networks. 2015 arXiv preprint arXiv:1503.00924.
57. Nam K, Sakai Y, Hashimoto Y, Kimura T, Kishida A. Fabrication of a heterostructural fibrillated collagen matrix for the regeneration of soft tissue function. Soft Matter. 2012; 8:472–480.
58. Chen, J., Kim, OV., Litvinov, R., Weisel, JW., Alber, MS., Chen, DZ. An automated approach for fibrin network segmentation and structure identification in 3D confocal microscopy images. 2014 IEEE 27th International Symposium on Computer-Based Medical Systems (CBMS); IEEE; 2014. p. 173-178.

Highlights

- Collagen-fibrin composite matrix exhibits synergistic mechanical properties
- Viscoelastic properties of compressed matrices reveal softening-stiffening behavior
- Material enhancements of fibrin-collagen composite have structural origin
- Compressive response of fibrous networks depends on protein concentration

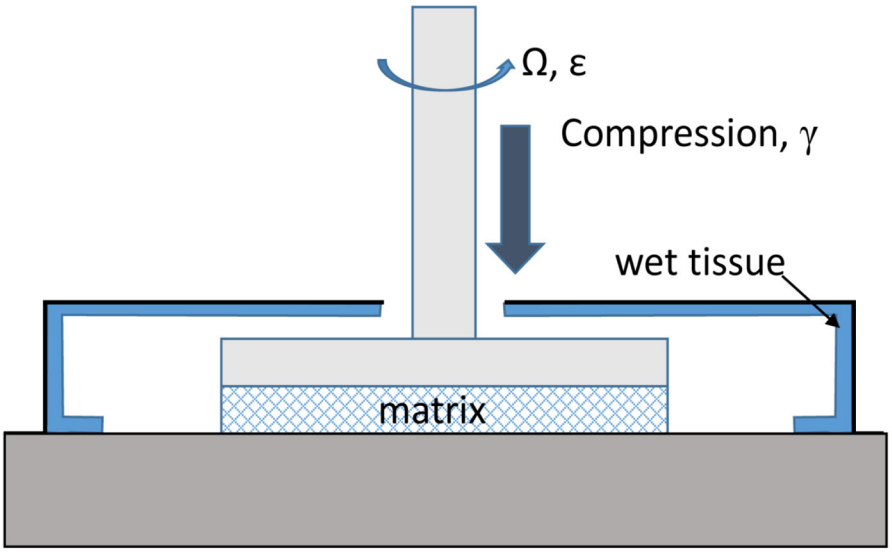

Figure 1.
Schematic diagram of the experimental procedure to measure shear viscoelastic response of compressed fibrin, collagen, or fibrin-collagen matrices.

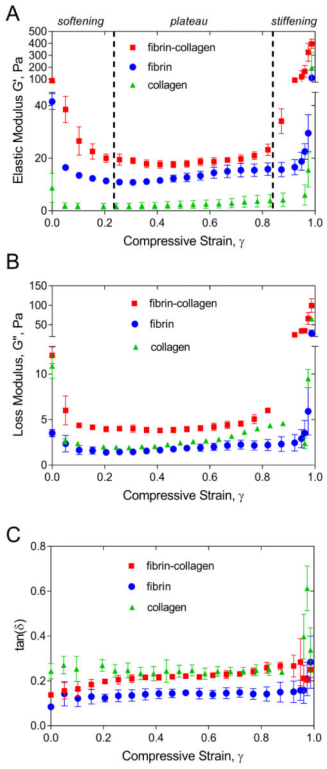

Figure 2.

A, B, C The elastic or storage modulus G′ (**A**), the loss or viscous modulus G″ (**B**), and the viscosity/elasticity ratio [tan(δ)= G″/ G′] as a function of compressive strain for the fibrin-collagen, fibrin, and collagen networks. Fibrin matrix was formed from two-fold diluted human platelet-poor plasma (fibrinogen concentration 2–3.5 mg/mL) and the final collagen concentration was 1.5 mg/mL. Each curve is an average over three samples prepared and measured under the same conditions (M±SD).

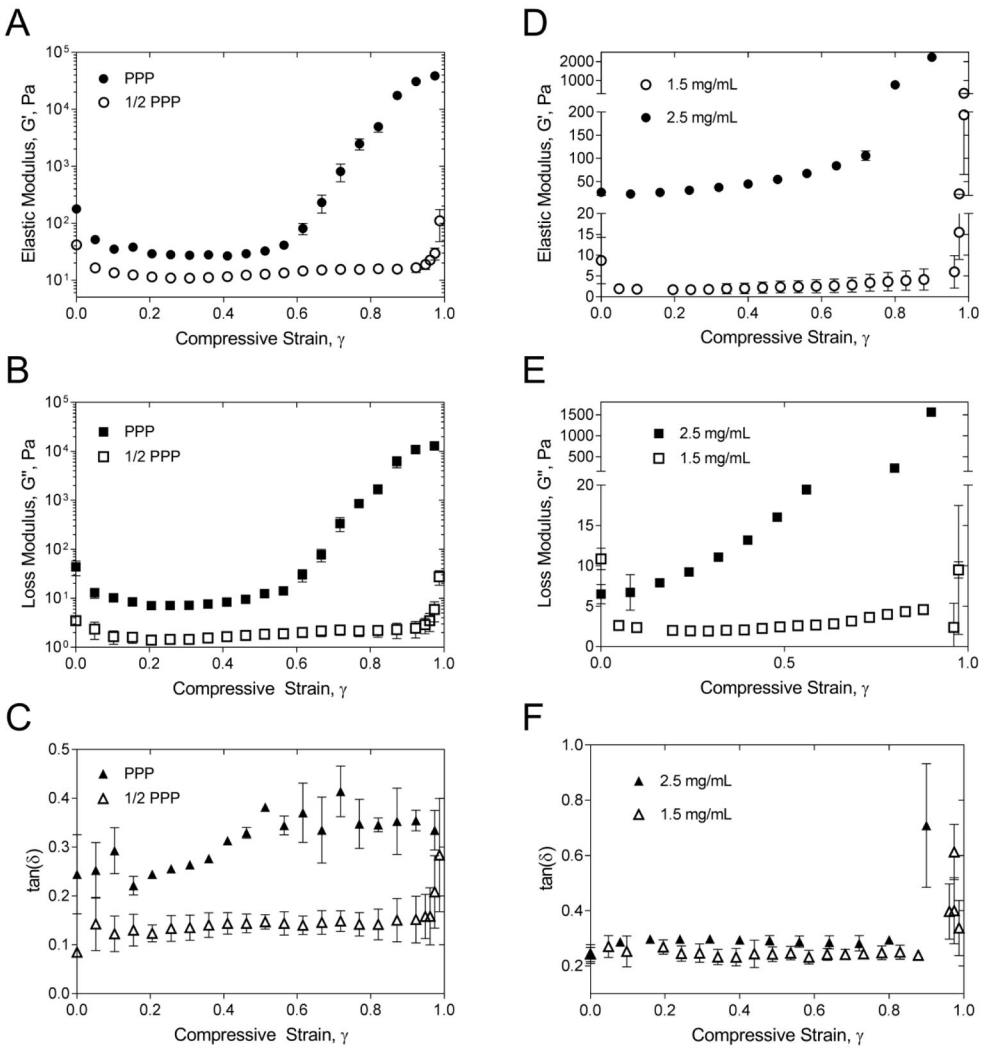

Figure 3.

A, B, C The elastic or storage modulus G′ (**A**), the loss or viscous modulus G″ (**B**), and the viscosity/elasticity ratio [tan (δ)=G″/G′], (**C**) as a function of compressive strain for the fibrin clots formed from undiluted (fibrinogen concentration 2–3.5 mg/mL) and diluted (fibrinogen concentration 1–1.75 mg/mL) platelet-poor plasma (PPP). **D, E, F:** The elastic or storage modulus G′, (**D**), the loss or viscous modulus G″, (**E**), and viscosity/elasticity ratio (**F**) as a function of compressive strain for the collagen network at two different protein concentrations, 1.5 mg/ml and 2.5 mg/ml. Each curve is an average over three collagen samples prepared and measured under the same conditions (M±SD).

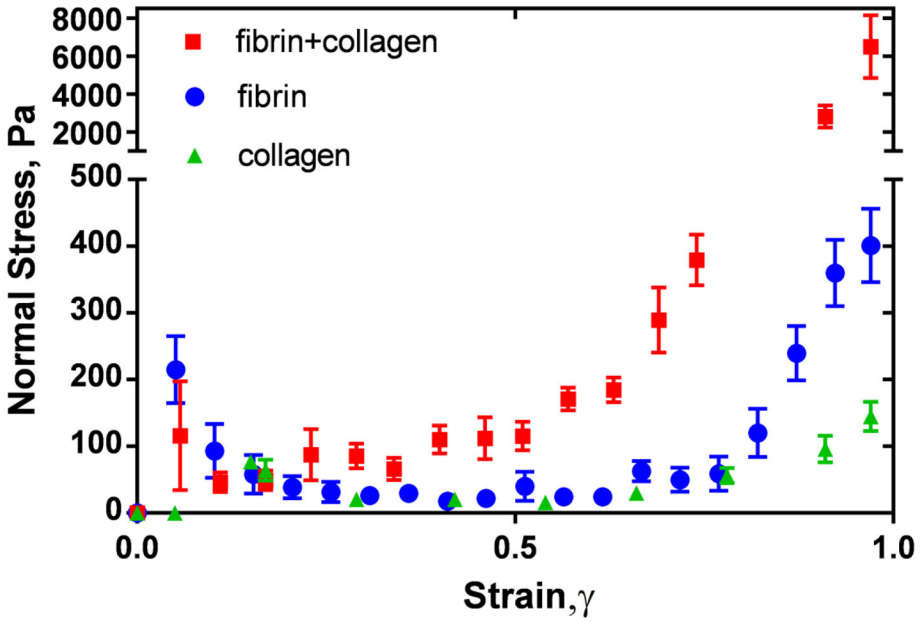

Figure 4.

Normal stress as a function of compressive strain for fibrin-collagen, fibrin, and collagen networks. Fibrin matrix was formed from two-fold diluted human platelet-poor plasma (fibrinogen concentration 2–3.5 mg/mL) and the final collagen concentration was 1.5 mg/mL. Each curve is an average over three constructs prepared and measured under the same conditions (M±SD).

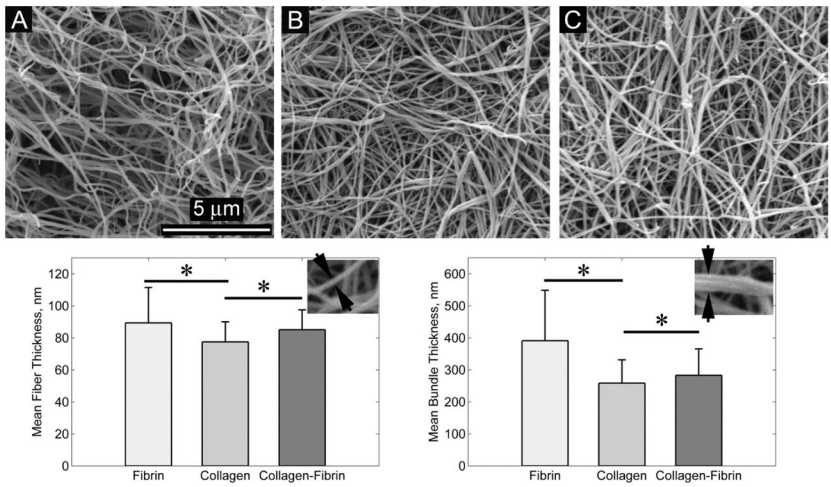

Figure 5.

Scanning electron microscopy images of fibrin (**A**) collagen (**B**) and fibrin-collagen (**C**) matrices compressed to more than 1/10th of their initial thickness. **D**, **E**: Quantitative measurements of collagen, fibrin and mixed scaffolds: (**D**) the mean diameter of individual fibers (M±SD) and (**E**) the mean thickness of fiber bundles (M±SD). An asterisk (*) is used to indicate the statistical difference when compared with collagen gel (two-tailed Mann-Whitney test, $P<0.05$, $n = 220$). The final fibrinogen and collagen concentrations were 2–3.5 mg/mL and 1.5 mg/mL, respectively (see also Supplementary Figure S2 and Figure S3).

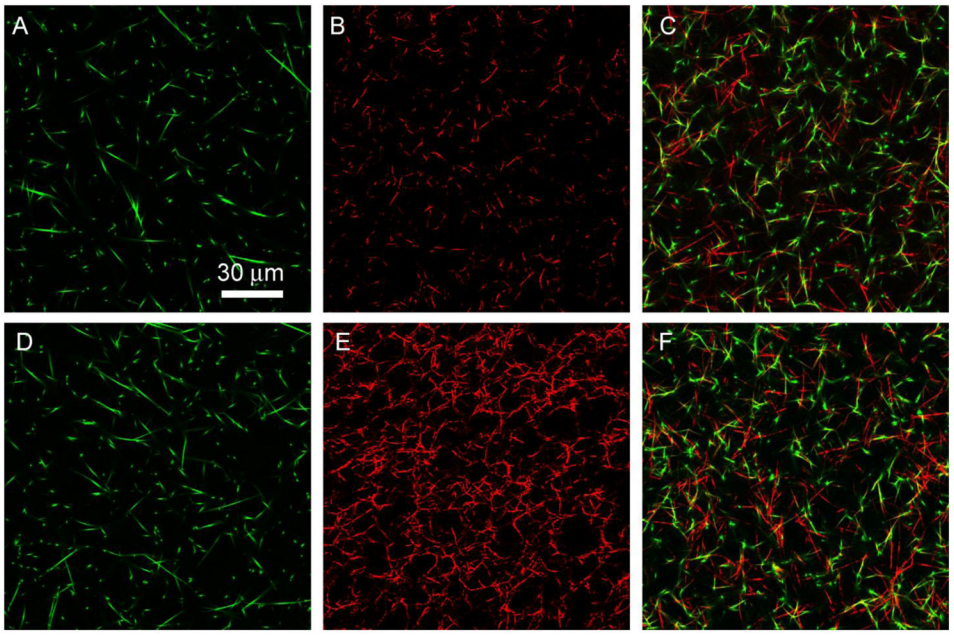

Figure 6.

Confocal microscopy images of uncompressed (top) and compressed (bottom) fibrin (**A**, **D**), collagen (**B**, **E**), and composite (**C**, **F**) matrices shown as confocal z-stack slices of 3D networks. Images of compressed networks were taken at a compressive strain γ=0.5. Collagen was imaged in reflection mode (red) and fluorescently labeled fibrin was visualized using fluorescence mode (green). The final fibrinogen and collagen concentrations were 2–3.5 mg/mL and 1.5 mg/mL, respectively (see also Supplementary Figure S4 and Figure S5).

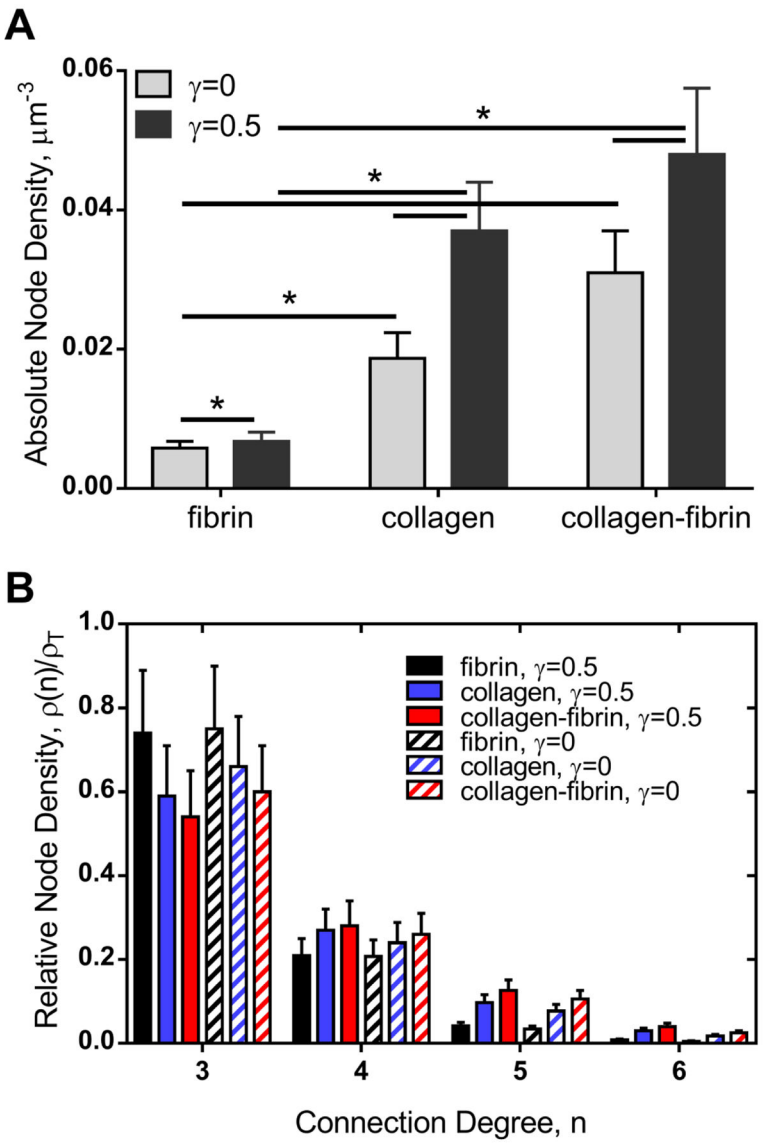

Figure 7.

A: Absolute node density for uncompressed (γ=0) and two-fold compressed (γ=0.5) networks of individually prepared fibrin and collagen matrices and fibrin-collagen fibers in the composite (M±SD); **P*<0.05, 1000 nodes in 3 samples, two-tailed Mann-Whitney test.

B: Connectivity distribution in terms of true and apparent branching points resulted from oblique impact of fibers. Here, ρ_T is the absolute node density of the network and n is the number of fibers irradiating from true or apparent branching points: true branching points (n=3), criss-crossing points (n=4), and their superposition (n=5 and n=6). Each symbol is an average over three different regions of a network (M±SD). Fibrin matrix was formed from two-fold diluted human platelet-poor plasma (fibrinogen concentration 2–3.5 mg/mL) and the final collagen concentration was 1.5 mg/mL.

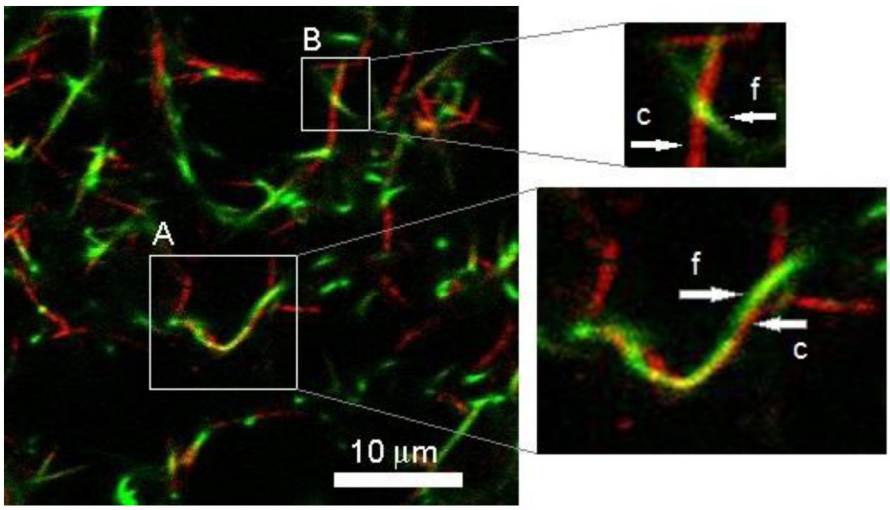

Figure 8.

A confocal microscopy image of the fibrin-collagen composite network exhibiting bundling (**A**) and criss-crossing (**B**) of fibers in the compressed matrix (γ=0.5). Here, '***c***' stands for collagen and '***f***' indicates fibrin fibers. The final fibrinogen and collagen concentrations were 2–3.5 mg/mL and 1.5 mg/mL, respectively.

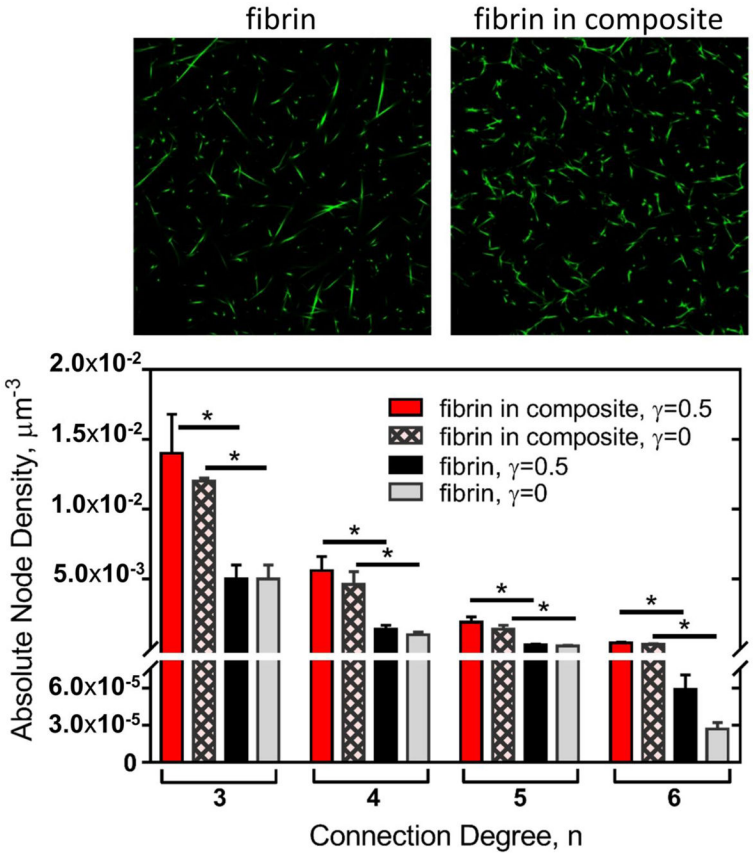

Figure 9.

Bottom: The absolute node density as a function of the node connection degree, n, in uncompressed and two-fold compressed fibrin networks formed from diluted plasma and in the presence of collagen (fibrin-collagen composite). Here, n is the number of fibers irradiating from true or apparent branching points: true branching points (n=3), criss-crossing points (n=4), and their superposition (n=5, 6). Each bar is an average over three different regions of a network (M±SD); *P<0.05, 1000 nodes in 3 samples, two-tailed Mann-Whitney test. **Top**: Confocal microscopy images of the uncompressed fibrin network in the absence (fibrin) and presence of collagen (fibrin in composite). Fibrin matrix was formed from two-fold diluted human platelet-poor plasma (fibrinogen concentration 2–3.5 mg/mL) and the final collagen concentration was 1.5 mg/mL.

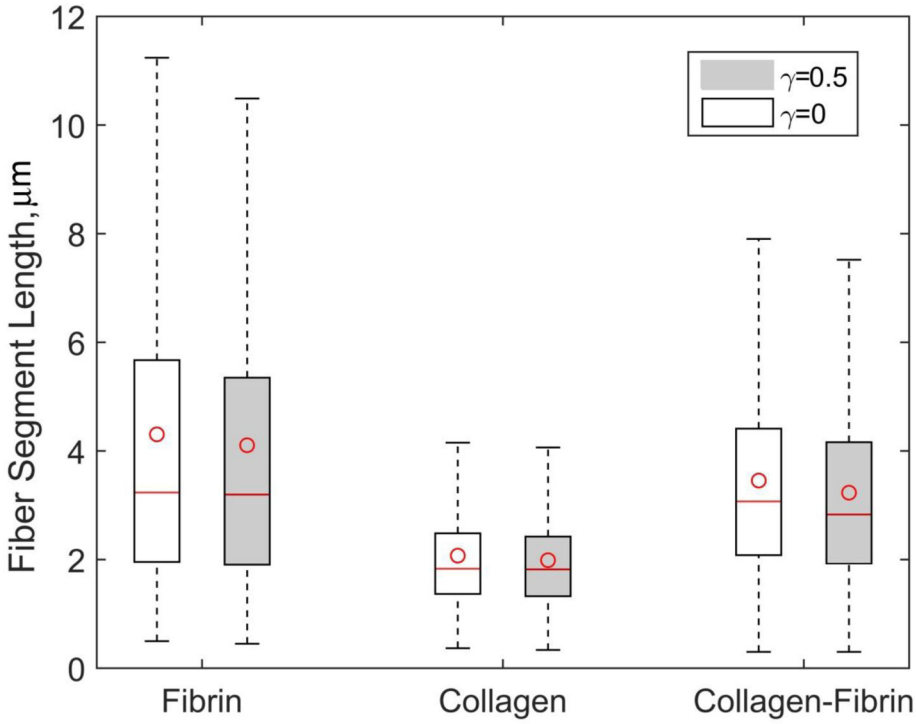

Figure 10.

Fiber segment length variations in uncompressed (γ=0) and compressed (γ=0.5) fibrin, collagen and fibrin-collagen networks. The box shows the interquartile range, a line in the box marks the median, whiskers indicate minimum and maximum values and the circle in the box shows the mean value. Fibrin matrix was formed from two-fold diluted human platelet-poor plasma (fibrinogen concentration 2–3.5 mg/mL) and the final collagen concentration in collagen and fibrin-collagen constructs was 1.5 mg/mL. Differences are statistically significant when compared to uncompressed matrices and collagen samples (P<0.01, 1200 segments in 3 samples, two-tailed Mann-Whitney test).